

# Effects of climate change on gilthead seabream aquaculture in the Mediterranean

Ines Haberle<sup>1,a</sup>, Domagoj K. Hackenberger<sup>2,a</sup>, Tamara Djerdj<sup>2</sup>, Lav Bavčević<sup>3</sup>, Sunčana Geček<sup>1</sup>, Branimir K. Hackenberger<sup>2</sup>, Nina Marn<sup>1,4</sup>, Jasminka Klanjšček<sup>1</sup>, Marija Purgar<sup>1</sup>, Jadranka Pečar Ilić<sup>1</sup>, and Tin Klanjscek<sup>1,\*</sup>

<sup>1</sup> Ruđer Bošković Institute, Bijenička cesta 54, 10002 Zagreb, Croatia

<sup>2</sup> Department of Biology, Josip Juraj Strossmayer University of Osijek, 31000 Osijek, Croatia

<sup>3</sup> Department of Ecology, Agriculture and Aquaculture, University of Zadar, M. Pavlinovića 1, 23000 Zadar, Croatia

<sup>4</sup> School of Biological Sciences, The University of Western Australia, Crawley WA 6009, Australia

<sup>a</sup> Equally contributing authors

\* Corresponding author: tin@irb.hr (Tin Klanjscek)

This is the accepted version of the following article:

Haberle, I., Hackenberger, D.K., Djerdj, T., Bavčević, L., Geček, S., Hackenberger, B.K., Marn, N., Klanjšček, J., Purgar, M., Pečar Ilić, J., Klanjscek, T. (2024) Effects of climate change on gilthead seabream aquaculture in the Mediterranean. *Aquaculture*, 578: 740052

published in the final form at <https://doi.org/10.1016/j.aquaculture.2023.740052>.

Available online 9 September 2023.

© 2023. This manuscript version is made available under the CC-BY-NC-ND 4.0 license <https://creativecommons.org/licenses/by-nc-nd/4.0>.

## Abstract

Aquaculture of gilthead seabream, arguably the most important finfish aquaculture species in the Mediterranean, faces changing environmental conditions due to faster-than-average climate change in the region. We utilize physiological modelling to estimate effects of moderate and severe climate change on key indices of aquaculture production for all coastal regions of the Mediterranean. Two publicly available global climate change scenarios with daily sea temperature projections serve as forcing for the physiological model during two-year farming cycles representing: (i) reference scenario starting in 2021, (ii) mid-term effects starting in 2051, and (iii) long-term effects starting in 2091.

We investigate effects of climate change by analyzing changes in time to fish reaching a market size, feed conversion ratio at the market size, and the weight of the fish and the associated feed conversion ratio after two years of farming. Additionally, we track the number of days with sea-water temperatures equal to or greater than 28 °C during the two-year period, when gilthead seabream starts experiencing temperature stress. Time to market size generally decreases with climate change from the initial average of 450 days for the reference period by up to 36 %. Feed conversion ratio at market size does not appreciably change with climate change, but it does change for the two-year culturing period for up to 10 %, primarily due to faster growth in warmer sea water, and the correspondingly greater weight achieved over the two-year growth cycle.

While the outlook for aquaculture is positive in the mid-term, some indicators show a negative trend in the long-term. The long-term effects of climate change will be greatest in the currently most productive farming regions of the Mediterranean: Levantine, Aegean, and Adriatic seas, and coastal waters of Tunisia. Our analysis focuses on basin-level features, but we provide geospatially referenced simulation results that can be used to analyze effects of climate change in a particular region of interest.

## Keywords

Dynamic Energy Budget, gilthead seabream *Sparus aurata*, Copernicus climate projection scenarios, feed conversion ratio, time to market

## 1 Introduction

Mediterranean region is the largest climate change hot-spot where warming up to 20 % higher than the global-average (Cherif et al., 2020), more frequent heatwave occurrence (Dayan et al., 2023), and substantial drying (Giorgi & Lionello, 2008; IPCC, 2021) modify marine ecosystems and jeopardize natural habitat suitability for many native species (Cavraro et al., 2022; Coma et al., 2009). The overall warming of the Mediterranean Sea and the increase in frequency of extreme events pose a risk to aquaculture production (FAO, 2022b) and related industries, thus endangering food security and sustainability of the blue economy. Given that the Mediterranean is also one of the 19 FAO major world fishing and aquaculture areas (Area 37; FAO 2023a), these risks also have global implications. Eastern Mediterranean in particular, where almost 93 % of the total regional aquaculture production takes place, is expected to suffer from severe and more frequent (marine) heat-waves, droughts, cold spells, extreme precipitations, and stronger winds (Dayan et al., 2023; Hochman et al., 2022; Makris et al., 2023). Related uncertainties of aquaculture performance decrease investor confidence, thus endangering ambitious plans for expanding aquaculture production integrated into global and regional sustainability initiatives, such as the United Nations (UN) Sustainable Development Goals, FAO Blue Transformation, and European Union (EU) Green Deal (EU Council, 2021; FAO, 2022a; Hambrey, 2017).

UN and EU strategies and directives prescribe a number of actions for mitigating impacts of climate change on aquaculture and boosting investor confidence. In particular, they advocate improved governance and regulations that foster implementation of best practices, development of new technologies through related scientific research, and optimization of cultivation practices to new environmental conditions (FAO, 2022b).

Selection of location and species plays an important role in aquaculture production: success depends on how well a particular species performs in environmental conditions dictated by the location. European sea bass (*Dicentrarchus labrax*, Moronidae) and gilthead seabream (*Sparus aurata*, Sparidae) constitute vast majority of Mediterranean finfish aquaculture (79 % in 2021; FAO 2023b). Gilthead seabream aquaculture reportedly poses lower environmental impact compared to the E. sea bass aquaculture (Zoli et al., 2023), while also being adapted to more temperate waters, as opposed to the cold thermal affinity of the E. sea bass (Adri.SmArtFish, 2020; Cavraro et al., 2022). These features favor gilthead seabream as a more suitable species when considering cultivation under global warming conditions. Quantifying effects of climate change on gilthead seabream aquaculture is therefore crucial for its future sustainable growth across the Mediterranean.

We use mechanistic modelling based on Dynamic Energy Budget (DEB) theory to quantify effects of future conditions on gilthead seabream aquaculture in the Mediterranean. In our approach, the DEB model predicts growth of fish as a function of local temperature predictions (C3S, 2020) based on the two representative climate change scenarios following IPCC RCP 4.5 and RCP 8.5 emission projections (IPCC, 2013). The growth curves are then used to estimate key aquaculture performance indicators:

1. **Time to market:** cultivation time when the fish reach 400 grams, the average weight of gilthead seabream typically sold at markets (Seginer & Ben-Asher, 2011). The indicator is important because it affects infrastructure and personnel costs needed to bring fish to marketable size for a given yearly production capacity.
2. **Feed conversion ratio (FCR) at 400 g:** since food constitutes up to 60 % of aquaculture production costs, changes in FCR can significantly impact production costs.
3. **Weight at 2 years:** because large fish is increasing in popularity, and a growth cycle rounded to a full year helps efficient use of infrastructure.
4. **FCR at 2 years:** to help estimate production costs of a two-year growth cycle.

Additionally, we look at two aggregate environmental indicators determining suitability for aquaculture production of gilthead seabream, and potentially other species:

1. **average temperature** as a proxy for warming, and
2. **number of days with water temperature equal to or above 28 °C**, the critical temperature above which gilthead seabream experiences increased stress and decreased growth.

We compare the key aquaculture performance and environmental indicators of gilthead seabream cohorts stocked in years 2021, 2051, and 2091 throughout the Mediterranean for moderate and worst-case warming scenarios, and discuss the implications.

## 2 Materials and Methods

### 2.1 Species

We focus our study on the gilthead seabream (*Sparus aurata*), one of the most important aquacultured species across the Mediterranean, and showing increased rearing potential in the Black Sea aquaculture (FAO, 2022b; Kaya Öztürk et al., 2020). Since the 1980s, gilthead seabream has

been cultivated primarily in intensive cage mariculture, which has almost completely replaced the traditional cultivation related to coastal sea pools and lagoons as natural fish trap systems (FAO, 2023c; Ravagnan, 1992). Due to the extremely high adaptability of this species to the conditions of intensive cultivation, its full breeding cycle can be entirely carried out ex-situ, i.e. within artificial facilities. Spawning and rearing of larvae and juveniles, up to a size of about 6.5 cm and weight of 3-5 grams, takes place under strictly controlled conditions, considering that these are the most sensitive life stages (Cardia & Lovatelli, 2015; FAO, 2023c). Thereafter, supplementary feeding and growth of larger juveniles and young adults up to the market size of about 400 g takes place in open cages (FAO, 2023c). Gilthead seabream performs best within its optimal thermal range of 20 to 25 °C and salinity of 25 to 40 PSU (Kaya Öztürk et al., 2020). Regardless of its eurithermal and euryhaline characteristics, significant increase in stress and reduction of growth occurs above 28 °C (Seginer & Ben-Asher, 2011), with reduction, or complete absence of feeding below 12 °C (Ibarz et al., 2003) and above 32 °C, and lethal temperatures of 5 °C and 34 °C (EFSA 2008a,b and references therein). Total production of gilthead seabream in the Mediterranean increased over 2.3 times in the last decade to over 300,000 tonnes in 2021, with a total production value of around 1.68 billion USD (FAO, 2023b).

## 2.2 Fish growth model

We use the principles of the Dynamic Energy Budget (DEB) theory to model the growth of cultivated fish. DEB describes flow of energy through an organism by mathematically describing its physiological processes - starting with the ingestion and assimilation of food from the environment to the processes of growth, maintenance, maturation and reproduction (Kooijman, 2010). The theory also accounts for organisms' responses to the environmental conditions, specifically temperature and food. Temperature ( $T$ ) dictates the growth and other metabolic rates, and its impact on the rate  $k(T)$  is integrated through the extended Arrhenius formulation (Kooijman, 2010), similar in form to the model of Schoolfield et al. (1981):

$$k(T) = \begin{cases} k_1 \cdot s_A(T), & \text{if } T < T_1 \\ k_1 \cdot s_A(T) \cdot s_H(T), & \text{if } T \geq T_1, \end{cases} \quad (1)$$

where  $k_1$  is metabolic rate at reference temperature  $T_1$ , relationship

$$s_A(T) = e^{T_A \left( \frac{1}{T_1} - \frac{1}{T} \right)}$$

represents classical Arrhenius formulation for correction of rate  $k_1$  at temperature  $T$ , and relationship

$$s_H(T) = \left(1 + e^{T_{AH}\left(\frac{1}{T_H} - \frac{1}{T_1}\right)}\right) \cdot \left(1 + e^{T_{AH}\left(\frac{1}{T_H} - \frac{1}{T}\right)}\right)^{-1}$$

accounts for the upper limit of the thermal tolerance range ( $T_A$  - Arrhenius temperature (K);  $T_H$  - upper boundary of the temperature tolerance range (K);  $T_{AH}$  - Arrhenius temperatures for the rate of decrease at upper boundary (K), see Table A.2).

Feed, as a source of energy, is given through a functional response  $f$ , a saturating function representing the feed density corresponding to starvation ( $f = 0$ ) up to ad libitum feeding ( $f = 1$ ). The functional response determines the actual feeding rate of the individual as a fraction of the size-specific maximal feeding rate. The model has the ability to simulate and track standard biometric measurements, length and weight, throughout the rearing process, thus allowing for determination of time-to-market. Weight, together with the information on ingested energy, also serves as a determinant of the FCR, where - in both terms of energy and weight - amount of input (feed) divided by the gain (produced fish) indicates conversion efficiency. Although a standard gilthead seabream harvest size (400 g) is usually reached before spawning, the rearing period may (depending on the rearing conditions) implicate reproduction events. DEB model explicitly captures the amount of energy invested into reproduction, and associated loss of weight due to spawning. The DEB parameter set for the model has been fitted based on the growth data obtained from the aquaculture, using the DEBtool software (DEBtool, 2023) with gilthead seabream AmP collection entry (Lika & Kooijman, 2016) as an initial parameter set. For a detailed description of the growth model and parameterization, see Supplement A.

### 2.3 Environmental variables

The simulations were performed for territorial coastal waters of Mediterranean countries extracted from Maritime Boundaries Geodatabase: Territorial Seas (12NM), Version 3. (Flanders Marine Institute, 2019, Belgium).

Daily average temperature projections were downloaded from Copernicus Climate Change Service (2020) for two Intergovernmental Panel for Climate Change (IPCC) Representative Concentration Pathway (RCP) emission scenarios: (i) RCP 4.5 as the moderate scenario, and (ii) RCP 8.5 as the worst-case scenario (IPCC, 2013). The IPCC RCP scenarios reflect the additional radiation (expressed in  $W/m^2$ ) in the year 2100 as a result of the greenhouse gases emission and other factors, compared to the pre-industrial era, causing changes in environmental temperature. Accordingly, a global average increase of 1.8°C and 3.7°C are expected for the RCP 4.5 and RCP 8.5, respectively (IPCC, 2014).

We assumed fish were fed slightly below ad libitum, a feeding strategy commonly used in aquaculture that avoids both under- and over-feeding while optimizing costs (Bonaldo et al., 2010; White, 2013). In DEB theory, this is represented by a constant functional response close to the maximum ( $f = 1$ ), typically  $f = 0.9$ . Using a constant  $f$  implies amount of ingested (and given) feed depends on the size of the organism, and the environmental temperature.

## 2.4 Simulations

We ran the simulations for three two-year rearing cycles (starting on April 1<sup>st</sup> in years 2021, 2051, and 2091), and two climate change scenarios (based on RCP 4.5 and 8.5), i.e. six simulation runs in total. Considering standard aquaculture practices, we assume the stocking fry was of adequate health with the common stocking size for gilthead seabream, 6.5 cm (EFSA, 2008a; Ökte, 2002), resulting in initial wet weight ( $W_{w_{init}}$ ) of 4.78 g. The stocking period (initial time for the simulation) and stocking size are also important factors affecting farming success. Modifying those is, however, out of the scope of our paper because we focus on the whole Mediterranean basin where optimal stocking time and size can vary wildly. The wide variability would reduce the ability to cross-compare results between regions and scenarios. Since we focus on differences rather than absolute values, we expect any locality bias to be (effectively) the same for all simulations, thus only marginally affecting the differences.

Simulations of the recent time period (starting in 2021) were used as a reference. Simulations starting in 2051 represent **mid-term impact** of climate change, while simulations for 2091 represent **long-term impact** of climate change. For consistency, Copernicus projection data were used for all simulations, including those of the recent time period (starting in 2021). Since temperature projections for RCP 4.5 and RCP 8.5 scenarios for the period 2021-2023 differ, the simulations starting in 2021 yield different results.

For each scenario, six indices were recorded at every spatial coordinate:

1. **Average temperature** as the average of all temperatures during the simulation period of two years.
2. **Number of days outside of the tolerance range** as the number of days with water temperature equal to or above 28 °C, the upper temperature limit beyond which gilthead seabream experiences stress and decreased growth (Kaya Öztürk et al., 2020). All days with daily average sea surface temperature equal or above 28 °C were counted.
3. **Time to market**, time at which the total fish weight reaches 400 grams, the typical market size used in Seginer & Ben-Asher (2011).

4. **FCR at 400 g** was calculated from feed ingestion recorded during simulations, using the ratio 
$$\text{FCR} = \frac{\text{total ingested energy (J)}}{\text{fish energy gain (J)}}.$$
5. **Total weight of fish at 2 years**, i.e. at the end of the simulation.
6. **FCR at 2 years** using the same approach as for FCR at 400 g, but for the full duration of the simulation.

Since the model tracks the dynamics of energy, we calculate the FCR as the ratio of ingested energy to energy within the fish gained during rearing. When the functional response ( $f$ ) is constant (as is the case in our simulations), the values of energy-based FCR is proportional to the commonly used FCR based on actual weights of feed and fish. The energy-based definition, however, offers a more universal measure of feed conversion because it assesses the ratio between ingested energy and the energy contained in the marketed fish directly, avoiding biases due to variable energy or water content of the feed. Details are presented in Supplement A.

To facilitate comparison with the commonly used FCR calculated from actual weights of feed and fish, we present effects of climate change on FCR in terms of ratios between expected future FCR and the FCR during the reference period (2021-2023). Since the constant of proportionality cancels out, the ratios are the same for all definitions of FCR, so the presented values are directly applicable to the commonly used weight-based FCR as well.

Mid-term effects of climate change on the indices were calculated as the difference in indices for each location between simulations starting in 2051, and simulations starting in 2021. Long-term effects of climate change on the indices were calculated as the difference in indices for each location between simulations starting in 2091, and simulations starting in 2021. Effects were calculated as differences in absolute values of indices, except for the FCR, which is presented relative to the reference period as described above. To help place the differences in context, we provide simulations of all indices, for all periods and scenarios, in the Supplementary Information, accompanied with basic statistics across all locations (mean, median, and 95<sup>th</sup> percentile) for each simulation. Spatially, simulations were run on a European Environmental Agency's (EEA) standard 10 km x 10 km grid of the Mediterranean Sea in territorial waters.

Simulations were coded in Python v3.10 programming language, using libraries for scientific computing, `Numpy` (Harris et al., 2020) and `SciPy` (Virtanen et al., 2020) as well as libraries for data analysis and manipulation `Pandas` (McKinney, 2010) and `GeoPandas` (Jordahl et al., 2020). Data analysis and visualization of the results were performed using the open source QGIS software (QGIS.org, 2023) and Matlab R2011b software (MATLAB, 2011).

### 3 Results

Simulations of all six scenarios are presented in the Supplementary Information (SI); comparisons are presented here. The overall increase in temperature due to climate change in the long-term is evident for both RCP scenarios, with the worst-case (RCP 8.5) having considerably warmer coastal waters than the moderate (RCP 4.5) scenario (Fig. 1, right panels). Mid-term simulations predict a lower overall increase in temperature for the worst-case (average of 0.33 °C), than the moderate (average of 0.55 °C) scenario; this is an artifact of using projections as a baseline (see discussion and Supplement C).

While sea temperatures are expected to rise throughout the Mediterranean, greatest sea warming, and therefore potential impacts of climate change on the performance indicators, are expected in the Northern Adriatic, Aegean and Levantine seas, and coasts of Tunisia and Libya (Figs. 1-4). In the long-term, the temperatures are expected to increase 2.39 °C on average for the RCP 8.5, 78 % more than the 1.34 °C increase expected for the RCP 4.5. Highest increases can be expected in the Northern Adriatic, for which the estimates for the long-term in RCP 8.5 range up to 3.79 °C. Areas of the Aegean Sea, Marmara Sea, Ligurian Sea, and Gulf of Lion also experience significant temperature increase (Fig. 1), but other indicators - particularly days with temperature above 28 °C - indicate continued suitability for gilthead seabream aquaculture.

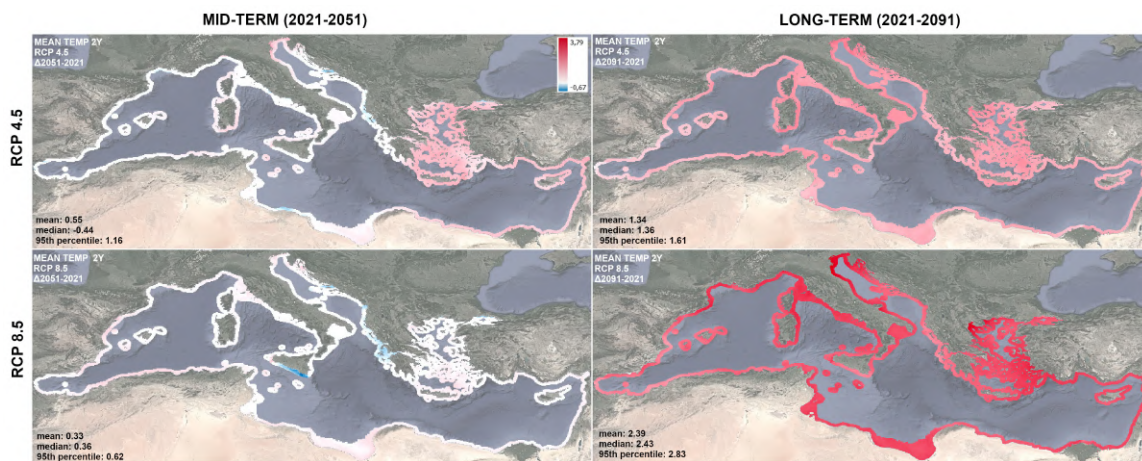


Figure 1: Differences in absolute values of average sea water temperature during a two-year rearing process in 2021 and 2051 (left), and 2021 and 2091 (right), for the IPCC RCP 4.5 (top) and 8.5 (bottom) scenarios. Red and blue colours indicate increase and decrease, respectively; white colour indicates no change. Mean, median, and 95<sup>th</sup> percentile change are indicated in the lower left corner of each plot.

The Levantine Sea, the Gulf of Gabes, and the Syrtis area alongside the coast of Libya will experience a marked increase in days of reduced suitability for gilthead seabream aquaculture ( $\geq 28$  °C; Fig. 2). The number of such days is greater for the RCP 8.5 than the RCP 4.5 in

both the mid- and long-term, despite the lower average temperature changes in the mid-term suggesting the contrary. Northern Adriatic may be experiencing the largest increases in average temperatures, but the number of days of reduced suitability for gilthead seabream cultivation will increase the most in the Gulf of Gabes, followed by the coastal waters of Libya. The absolute maximum of reduced suitability days is, however, predicted to remain in the North-East Levantine Sea, where it is expected to increase from a maximum of 129 in 2021, to 243 in 2091, for the RCP 8.5.

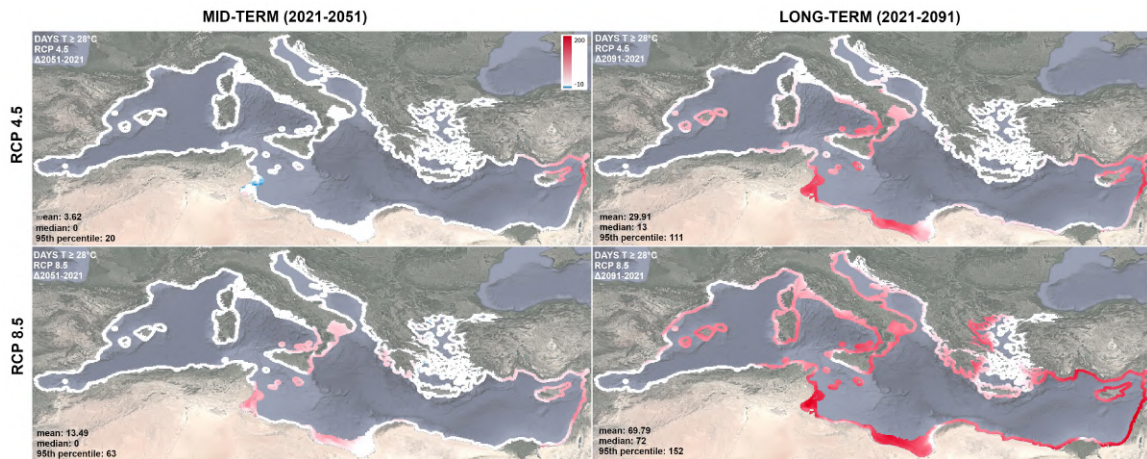


Figure 2: Differences in absolute values of number of days with temperature exceeding the upper thermal limit for non-stressed gilthead seabream growth (28 °C) within a two-year rearing period, between 2021 and 2051 (left), and 2021 and 2091 (right), for the IPCC RCP 4.5 (top) and 8.5 (bottom) scenarios. Red and blue colours indicate increase and decrease, respectively; white colour indicates no change. Mean, median, and 95<sup>th</sup> percentile change are indicated in the lower left corner of each plot.

In the long-term, the average time to market (Fig. 3) will decrease from 453 to 433 days for RCP 4.5, and from 443 to 418 days for the RCP 8.5. The greatest decreases are expected for the RCP 8.5, by the maximum of 161 days in the Gulf of Lion, followed by the Aegean, Adriatic and the Alboran Sea. Unexpectedly, the time to market will *increase* in the mid-term RCP 8.5 scenario in the areas of the central Mediterranean. However, this is compensated by the increased warming that will occur in the long-term, with the exception of the Levantine Sea, where time to market will remain prolonged for up to 66 days despite the warming. On average, a general decrease in time to market is expected to be cca. 21 and 25 days for the long-term RCP 4.5 and 8.5 simulation, respectively.

FCR at time-to-market shows very small changes between periods, with the maximum increase of approximately 0.24 % across all locations and scenarios (Fig. 4). The two-year FCR, however, shows a significant and varied response. Generally, the two-year FCR slightly increases, but there is a decrease in coastal areas of Tunisia and Libya, and the Levantine Sea (Fig. 5). The

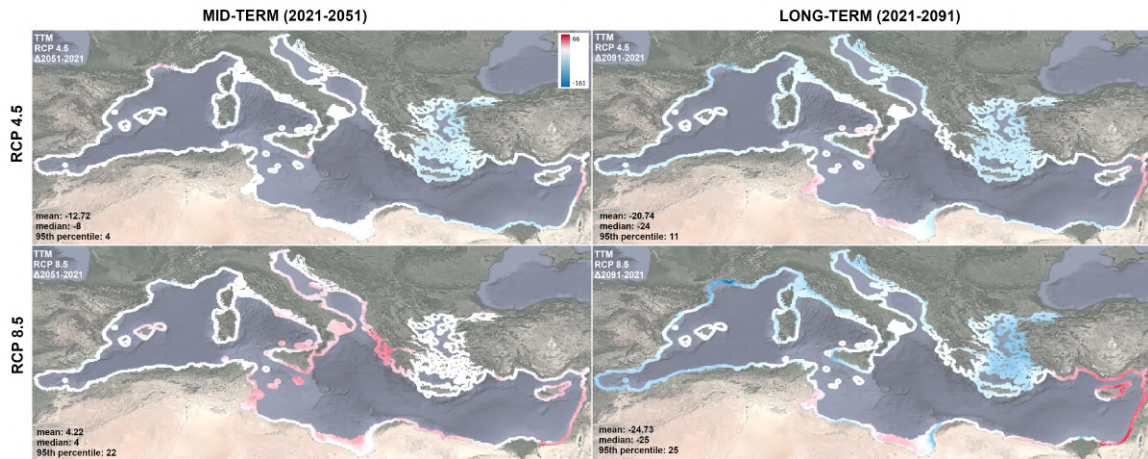


Figure 3: Differences in absolute values of time-to-market for gilthead seabream between rearing periods in 2021 and 2051 (left), and 2021 and 2091 (right), for the IPCC RCP 4.5 (top) and 8.5 (bottom) scenarios. Red and blue colours indicate increase and decrease, respectively; white colour indicates no change. Mean, median, and 95<sup>th</sup> percentile change are indicated in the lower left corner of each plot.

maximum increase relative to the baseline two-year FCR (Figures B.1 and B.4, bottom right) is 9.7 % and 10 % for the RCP 4.5 and the RCP 8.5, respectively. Changes in weight attained during two years of growth follows the same qualitative pattern; the average weight attained during the reference period is 1038 grams for the RCP 4.5 (Figure B.1, bottom left) and 1064 grams for the RCP 8.5 (Figure B.4, bottom left) with the increases by 9 % and 13% for the RCP 4.5 and RCP 8.5 in the long-term (Fig. 6), respectively.

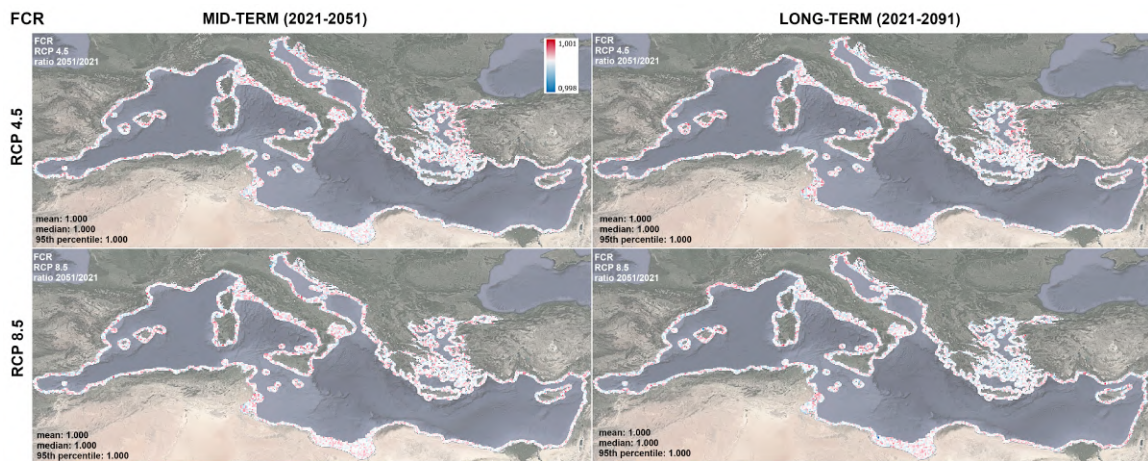


Figure 4: FCR relative to the reference period (2021-2023) at time-to-market (400 g) for gilthead seabream, for rearing starting in 2051 (left), and 2091 (right), for the IPCC RCP 4.5 (top) and 8.5 (bottom) scenarios. Red and blue colours indicate increase and decrease, respectively; white colour indicates no change. Mean, median, and 95<sup>th</sup> percentile change are indicated in the lower left corner of each plot.

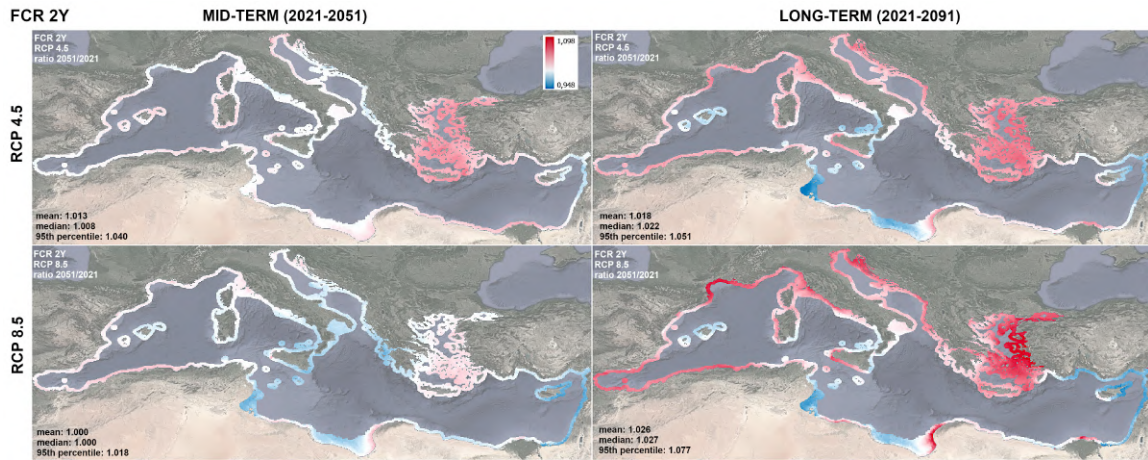


Figure 5: FCR at 2 years relative to the reference period (2021-2023) for gilthead seabream within a two-year rearing period starting in 2051 (left), and 2091 (right), for the IPCC RCP 4.5 (top), and 8.5 (bottom) scenarios. Red and blue colours indicate increase and decrease, respectively; white colour indicates no change. Mean, median, and 95<sup>th</sup> percentile change are indicated in the lower left corner of each plot.

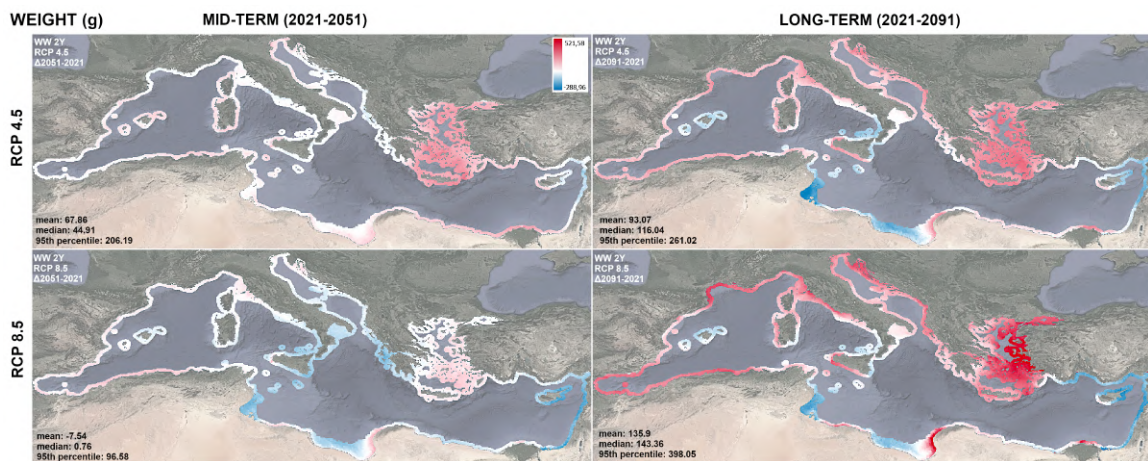


Figure 6: Differences in absolute values of weight after two years for gilthead seabream between rearing periods in 2021 and 2051 (left), and 2021 and 2091 (right), for the IPCC RCP 4.5 (top) and 8.5 (bottom) scenarios. Red and blue colours indicate increase and decrease, respectively; white colour indicates no change. Mean, median, and 95<sup>th</sup> percentile change are indicated in the lower left corner of each plot.

## 4 Discussion

We used physiological modelling and climate change projections to quantify the expected mid- and long-term effects of climate change on key performance indicators for gilthead seabream aquaculture in coastal areas of the Mediterranean. Here we focus on key features of the mid- and long-term effects of climate change to identify areas where environmental conditions are expected to significantly worsen. Simulation results included in the Supplemental Information enable further analysis.

Critically, most productive gilthead seabream aquaculture areas can expect the greatest impacts of climate change. Levantine, Aegean, the northern coast of the Adriatic Sea, and Gulf of Gabes account for majority of gilthead seabream aquaculture in the Mediterranean, with Turkey, Greece, Croatia, and Tunisia contributing with total of 71 % of global production (FAO, 2023b). These areas can expect the highest increase in temperature and/or number of days above the optimal range for gilthead seabream growth, implying that aquaculture in these regions might suffer from decrease in productivity the most. Hence, the sector needs to take climate change seriously.

Expectedly, stronger climate change will generally cause more pronounced effects. Surprisingly, however, the mid-term effects of climate change seem to be more severe for the RCP 4.5 than the RCP 8.5 scenario. For example, the mid-term RCP 8.5 scenario predicts a stagnation and even a decrease in the temperature and, consequently, an increase in time to market and two-year fish weight; all other scenarios generally predict an increase in temperature, a decrease in time to market, and an increase in weight of two-year old fish.

The apparent difference is an artifact of the reference scenario (simulations starting in 2021): RCP 8.5 results in more pronounced climate change projections in 2021 than RCP 4.5, so even though the climate change effects in 2051 are larger than for the RCP 4.5, the differences between the 2021 and 2051 are smaller. When RCP 4.5 baseline is used for estimating mid-term changes in RCP 8.5, the unexpected pattern disappears (Fig. C.1). The two scenarios (RCP 4.5 and RCP 8.5) differ quantitatively, but present the same qualitative results.

Weight and FCR over a two-year growth cycle have the same pattern: general increase as the climate change progresses, but a decrease in some areas of the southern Mediterranean and Levantine Sea. The increase in FCR is slight, mainly caused by the increase in the weight of the fish: while within tolerance range for any given period, fish will grow larger when temperatures are higher. Contrary to the rule, however, southern and Levantine Sea areas - experiencing the largest increases in temperatures - show a decline in two-year FCR. Extremely high temperatures

in those areas explain the discrepancy: temperature stress in those areas reduces fish growth and, therefore, FCR. Hence, the apparent reduction in FCR may not be beneficial to farmers: rearing cycles are longer, and temperature-stressed fish are more susceptible to diseases and other pressures.

A study limited to Greek coastal water and focusing on a different species, the European sea bass, showed similar trends in growth (Stavrakidis-Zachou *et al.*, 2021) as presented in our study: increased temperature resulted in faster growth. Authors further show that timing of stockings may also play an important role, and that extreme weather events pose a threat to both cage infrastructure and feeding regime integrity that could lead to significant losses in yields and profit. Indeed, optimal timing of stockings plays an important role in aquaculture production, and should be investigated in depth for any particular region of interest.

Our model assumes a constant functional response, i.e. level of feeding relative to the maximum feeding rate. Therefore, actual ingested energy (and feed) depends on the size of the fish, and temperature. For example, a gilthead seabream of 200 g will at 12 °C ingest only 41 % of the energy the same fish would ingest at 28 °C. We do not account for any additional changes in feeding practices, which can vary wildly between farms. Assuming equal feeding practices throughout the Mediterranean facilitates spatial comparisons by reducing bias due to specifics of aquaculture facilities and their technology. This results in a more optimistic baseline FCR than reality because farmers may reduce feeding during cold periods even further than assumed in our model, e.g. to avoid the winter disease, or due to bad weather. If feeding were further reduced, the fish would grow more slowly, thereby increasing the FCR. Warmer winters predicted by the climate scenarios will reduce the problems related to cold seasons and should, at least in colder regions, improve (reduce) FCR. Consequently, our predictions are conservative: in cold regions, a greater positive effect of climate change is expected.

Even though FCR is usually calculated as the ratio of actual weights of spent feed and produced fish, we based our calculations on the ratio of energies (ingested energy vs. energy content of fish). Energy-based FCR (i) is consistent with the model because it uses state variables directly, thus also (ii) avoiding bias due to water and/or energy content of the feed. Since feed quality and water content varies between feed producers, we suggest energy-based FCR would facilitate comparisons between feeds and even potentially species. Therefore, the energy-based FCR might be a better standard for the aquaculture industry than the existing, weight-based one. Since the effects of climate change are represented in terms of FCR ratios, the values reported in Figs. 4 and 5 are directly applicable to all definitions of FCR.

Climate change also affects abiotic factors other than the temperature, such as salinity, pH,

and oxygen levels. Current salinity in the Mediterranean can already be close to or above 38 PSU, which causes a reduction in gilthead seabream growth (Lotfy *et al.*, 2021). Increases in temperature and salinity also both decrease oxygen solubility in seawater (Song *et al.*, 2019), thus limiting oxygen availability. Together with increase of fish metabolism and oxygen demand at higher temperatures (Remen *et al.*, 2015), these parallel processes can lead to oxygen undersaturation, and negatively affect both fish growth and their feed conversion efficiency.

Biotic factors such as algal blooms and pathogen outbreaks are also expected to increase (Wells *et al.*, 2015), thus posing additional risks to fish, and therefore aquaculture production and profitability (Hoagland & Scatasta, 2006). Aquaculture production and the related Mediterranean socio-ecological systems and governance is expected to suffer from these challenges (Bednarsek *et al.*, 2023), so appropriate and timely actions are needed to ensure the sustainable development of the sector. Unfortunately, comprehensive basin-wide quantitative mid- and long-term predictions for the effects of aforementioned (a)biotic factors on aquaculture production in the context of climate change do not yet exist.

In general, warming conditions show a beneficial effect for growth of gilthead seabream resulting in shorter time-to-market, and larger fish sizes for a given culturing period. Therefore, productivity of gilthead seabream aquaculture may actually increase, especially in the mid-term. However, the increase in number of days with temperature outside of the tolerance range ( $\geq 28$  °C) indicates that some of the currently most productive regions may require a shift towards species with even higher temperature tolerance, or a bio-engineered (e.g. through selection) gilthead seabream stock. Alternatively, gilthead seabream aquaculture could shift to areas with more suitable future conditions, such as the western Mediterranean. Due to the higher temperature tolerance range of gilthead seabream compared to that of E. sea bass, farmers might consider shifting production from E. sea bass to gilthead seabream, at least in the mid-term.

## 5 Conclusion

This study shows that climate change will have a significant impact on Mediterranean gilthead seabream aquaculture, with the most productive regions today being the most affected. While warming generally leads to shorter time-to-market, and larger fish sizes if the rearing time is fixed, extreme temperatures can cause stress in certain areas, leading to lower growth and increased susceptibility to disease. Adaptation to climate change is therefore crucial for the sustainable development of aquaculture in the Mediterranean. Possible adaptation strategies include switching to species with higher temperature tolerance, using engineered seabream stocks, adapting stocking timing to minimize the number of warm days, and/or relocating aquaculture to areas

with more suitable future conditions such as the western Mediterranean. Furthermore, appropriate and timely measures to mitigate and adapt aquaculture production to changing climate conditions are crucial for maintaining and management of socio-ecological systems/relationships in the region.

## CRedit authorship contribution statement

**Ines Haberle:** Conceptualization, Formal analysis, Methodology, Software, Visualisation, Writing - original draft, Writing - review and editing. **Domagoj K. Hackenberger:** Investigation, Methodology, Software, Writing - original draft. **Tamara Djerdj:** Data curation, Investigation. **Lav Bavčević:** Conceptualization, Methodology. **Sunčana Geček:** Formal analysis, Writing - review and editing. **Branimir K. Hackenberger:** Funding acquisition, Resources, Supervision, Writing - review and editing. **Nina Marn:** Methodology, Writing - review and editing. **Jasminka Klanjšček:** Methodology, Writing - review and editing. **Marija Purgar:** Data Curation, Investigation. **Jadranka Pečar Ilić:** Software. **Tin Klanjscek:** Conceptualization, Funding acquisition, Project administration, Supervision, Writing - original draft, Writing - review and editing.

## Acknowledgment

IH and MP were funded by the Croatian Science Foundation (HRZZ) through *Young Researchers' Career Development Project*, DOK-2018-09-4671 and DOK-2021-02-6688. This work has been fully supported through the HRZZ grant IP-2018-01-3150-AqADAPT to TK.

## Conflict of Interest Statement

All authors declare no conflict of interest.

## Data Availability Statement

The data and code underlying the findings of this study are openly available at Zenodo, <https://doi.org/10.5281/zenodo.8325033>.

## References

- Adri.SmArtFish (2020). Report on SSF vulnerability to Climate Change in GSA17. Deliverable D3.3.1., Evaluation of the small-scale fishing sector, Interreg project Adri.SmArtFish.
- Bednarsek, N., Guilloux, B., Canu, D. M., Galdies, C., Guerra, R., Simoncelli, S., Feely, R. A., Pelletier, G., Gašparović, B., Godrijan, J., Malej, A., Solidoro, C., Turk, V., Zunino, S., Bednarsek, N., Guilloux, B., Canu, D. M., Zunino, S., & Guerra, R. (2023). Ocean Acidification as a Governance Challenge in the Mediterranean Sea: Impacts from Aquaculture and Fisheries. In *Ocean Governance* (pp. 403–432). MARE Publication Series, German Institute of Development and Sustainability (IDOS). [https://doi.org/10.1007/978-3-031-20740-2\\\_18](https://doi.org/10.1007/978-3-031-20740-2\_18).
- Bonaldo, A., Isani, G., Fontanillas, R., Parma, L., Grilli, E., & Gatta, P. P. (2010). Growth and feed utilization of gilthead sea bream (*Sparus aurata*, L.) fed to satiation and restrictively at increasing dietary energy levels. *Aquaculture international*, 18, 909–919. <https://doi.org/10.1007/s10499-009-9312-0>.
- C3S (2020). Climate Data Store: Marine biogeochemistry data for the Northwest European Shelf and Mediterranean Sea from 2006 up to 2100 derived from climate projections. Copernicus Climate Change Service (C3S) Climate Data Store (CDS). <https://doi.org/10.24381/cds.dcc9295c>. Accessed on 29.04.2023.
- Cardia, F., & Lovatelli, A. (2015). Aquaculture operations in floating HDPE cages: A field handbook. *FAO Fisheries and Aquaculture Technical Paper, No. 593*. FAO and Ministry of Agriculture of the Kingdom of Saudi Arabia.
- Cavraro, F., Anelli Monti, M., Matić-Skoko, S., Caccin, A., & Pranovi, F. (2022). Vulnerability of the small-scale fishery to climate changes in the northern-central Adriatic Sea (Mediterranean Sea). *Fishes*, 8, 9. <https://doi.org/10.3390/fishes8010009>.
- Cherif, S., Doblaz-Miranda, E., Lionello, P., Borrego, C., Giorgi, F., Iglesias, A., Jebari, S., Mahmoudi, E., Moriondo, M., Pringault, O., Rilov, G., Somot, S., Tsikliras, A., Vila, M., & G, Z. (2020). Drivers of change. In *Climate and environmental change in the Mediterranean basin – current situation and risks for the future* (pp. 59–180). Union for the Mediterranean, Plan Bleu, UNEP/MAP, Marseille, France. <https://doi.org/10.5281/zenodo.7100601>.
- Coma, R., Ribes, M., Serrano, E., Jiménez, E., Salat, J., & Pascual, J. (2009). Global warming-enhanced stratification and mass mortality events in the Mediterranean. *Proceedings of the National Academy of Sciences*, 106, 6176–6181. <https://doi.org/10.1073/pnas.0805801106>.
- Dayan, H., McAdam, R., Juza, M., Masina, S., & Speich, S. (2023). Marine heat waves in the Mediterranean Sea: An assessment from the surface to the subsurface to meet national needs. *Frontiers in Marine Science*, 10, 142. <https://doi.org/10.3389/fmars.2023.1045138>.

- DEBtool (2023). Software package DEBtool\_M. [https://github.com/add-my-pet/DEBtool\\_M](https://github.com/add-my-pet/DEBtool_M).
- EFSA (2008a). Animal welfare aspects of husbandry systems for farmed European seabass and gilthead seabream - Scientific Opinion of the Panel on Animal Health and Welfare. *The EFSA Journal*, 6, 1–21.
- EFSA (2008b). Scientific report of EFSA prepared by Working Group on seabass/seabream welfare on Animal Welfare Aspects of Husbandry Systems for Farmed European seabass and gilthead seabream. Annex I to The EFSA Journal(2008) 844. European Food Safety Authority.
- EU Council (2021). Strategic guidelines for a more sustainable and competitive EU aquaculture for the period 2021 to 2030. COM(2021) 236 final. <https://eur-lex.europa.eu/legal-content/EN/TXT/?uri=COM:2021:236:FIN>.
- FAO (2022a). Blue transformation - roadmap 2022–2030: A vision for fao’s work on aquatic food systems. <https://doi.org/10.4060/cc0459en>.
- FAO (2022b). *The State of World Fisheries and Aquaculture 2022. Towards Blue Transformation*. Food and Agriculture Organization of the United Nations. <https://doi.org/10.4060/cc0461en>.
- FAO (2023a). FAO major fishing areas. Accessed via <https://www.fao.org/fishery/en/area> on 24.04.2023. Coordinating Working Party on Fishery Statistics (CWP). Fishing Areas for Statistical Purposes.
- FAO (2023b). Fishery and Aquaculture Statistics. Global production by production source 1950-2021 (FishStatJ). In *FAO Fisheries and Aquaculture Division [online]*. Rome: FAO Fisheries and Aquaculture Department. Updated 2023. FishStatJ software available at: <https://www.fao.org/fishery/en/topic/166235>.
- FAO (2023c). Sparus aurata. cultured aquatic species information programme. [https://www.fao.org/fishery/en/culturedspecies/sparus\\_aurata/en](https://www.fao.org/fishery/en/culturedspecies/sparus_aurata/en). Text by Colloca, F.; Cerasi, S.. Fisheries and Aquaculture Division [online]. Updated 2005-05-17. Rome. Accessed 20.04.2023.
- Flanders Marine Institute (2019). Maritime Boundaries Geodatabase: Territorial Seas (12NM) - Dataset. VLIZ, Belgium. <http://www.vliz.be/en/imis?dasid=6319&doiid=387>. <https://doi.org/10.14284/387>.
- Giorgi, F., & Lionello, P. (2008). Climate change projections for the Mediterranean region. *Global and planetary change*, 63, 90–104. <https://doi.org/10.1016/j.gloplacha.2007.09.005>.
- Hambrey, J. (2017). The 2030 Agenda and the sustainable development goals: the challenge for aquaculture development and management. *FAO Fisheries and Aquaculture Circular*, .
- Harris, C. R., Millman, K. J., van der Walt, S. J., Gommers, R., Virtanen, P., Cournapeau, D., Wieser, E., Taylor, J., Berg, S., Smith, N. J., Kern, R., Picus, M., Hoyer, S., van Kerkwijk, M. H., Brett, M., Haldane, A., del Río, J. F., Wiebe, M., Peterson, P., Gérard-Marchant, P., Sheppard, K., Reddy, T.,

- Weckesser, W., Abbasi, H., Gohlke, C., & Oliphant, T. E. (2020). Array programming with NumPy. *Nature*, *585*, 357–362. <https://doi.org/10.1038/s41586-020-2649-2>.
- Hoagland, P., & Scatasta, S. (2006). The economic effects of harmful algal blooms. (pp. 391–402). Berlin/Heidelberg, Germany: Springer.
- Hochman, A., Marra, F., Messori, G., Pinto, J. G., Raveh-Rubin, S., Yosef, Y., & Zittis, G. (2022). Extreme weather and societal impacts in the eastern Mediterranean. *Earth System Dynamics*, *13*, 749–777.
- Ibarz, A., Fernández-Borràs, J., Blasco, J., Gallardo, M., & Sánchez, J. (2003). Oxygen consumption and feeding rates of gilthead sea bream (*Sparus aurata*) reveal lack of acclimation to cold. *Fish Physiology and Biochemistry*, *29*, 313–321. <https://doi.org/10.1007/s10695-004-3321-8>.
- IPCC (2013). *Summary for Policymakers*. Cambridge University Press, Cambridge, United Kingdom and New York, NY, USA.
- IPCC (2014). Climate Change 2013: The Physical Science Basis. In Core Writing Team, R. Pachauri, & L. Meyer (Eds.), *Contribution of Working Group I to the Fifth Assessment Report of the Intergovernmental Panel on Climate Change*. IPCC, Geneva, Switzerland, 151p.
- IPCC (2021). Summary for Policymakers. In V. Masson-Delmotte, P. Zhai, A. Pirani, S. Connors, C. Péan, S. Berger, N. Caud, Y. Chen, L. Goldfarb, M. Gomis, M. Huang, K. Leitzell, E. Lonnoy, J. Matthews, T. Maycock, T. Waterfield, O. Yelekçi, R. Yu, & B. Zhou (Eds.), *Climate Change 2021: The Physical Science Basis. Contribution of Working Group I to the Sixth Assessment Report of the Intergovernmental Panel on Climate Change*. Intergovernmental Panel on Climate Change, Switzerland.
- Jordahl, K., den Bossche, J. V., Fleischmann, M., Wasserman, J., McBride, J., Gerard, J., Tratner, J., Perry, M., Badaracco, A. G., Farmer, C., Hjelle, G. A., Snow, A. D., Cochran, M., Gillies, S., Culbertson, L., Bartos, M., Eubank, N., maxalbert, Bilogur, A., Rey, S., Ren, C., Arribas-Bel, D., Wasser, L., Wolf, L. J., Journois, M., Wilson, J., Greenhall, A., Holdgraf, C., Filipe, & Leblanc, F. (2020). geopandas/geopandas: v0.8.1. URL: <https://doi.org/10.5281/zenodo.3946761>. <https://doi.org/10.5281/zenodo.3946761>.
- Kaya Öztürk, D., Öztürk, R., Baki, B., Karayücel, I., & Karayücel, S. (2020). Monthly variation of growth, biochemical composition, fatty and amino acids patterns of gilthead sea bream (*Sparus aurata*) in offshore cage systems under brackish water conditions in the Black Sea. *Aquaculture Research*, *51*, 4961–4983. <https://doi.org/10.1111/are.14833>.
- Kooijman, S. A. L. M. (2010). *Dynamic Energy Budget theory for metabolic organisation*. Cambridge: Cambridge University Press.

- Lika, D., & Kooijman, B. (2016). AmP *Sparus aurata*, version 2016/10/15. [https://www.bio.vu.nl/thb/deb/deblab/add\\_my\\_pet/entries\\_web/Sparus\\_aurata/Sparus\\_aurata\\_res.html](https://www.bio.vu.nl/thb/deb/deblab/add_my_pet/entries_web/Sparus_aurata/Sparus_aurata_res.html). Accessed on 30.04.2023.
- Lotfy, A. M., Elhetawy, A. I. G., Habiba, M. M., & Abdel-Rahim, M. M. (2021). A comparative study on the effects of seawater and underground saltwater on water quality, growth, feed utilization, fish biomass, digestive system development, and blood health in gilthead seabream, *Sparus aurata*. *AACL Bioflux*, 14. <http://www.bioflux.com.ro/aac1>.
- Makris, C. V., Tolika, K., Baltikas, V. N., Velikou, K., & Krestenitis, Y. N. (2023). The impact of climate change on the storm surges of the Mediterranean Sea: Coastal sea level responses to deep depression atmospheric systems. *Ocean Modelling*, 181, 102149. <https://doi.org/10.1016/j.ocemod.2022.102149>.
- MATLAB (2011). Version 7.13 (R2011b). The MathWorks Inc., Natick, Massachusetts.
- McKinney, W. (2010). Data Structures for Statistical Computing in Python. In Stéfan van der Walt, & Jarrod Millman (Eds.), *Proceedings of the 9th Python in Science Conference* (pp. 56 – 61). <https://doi.org/10.25080/Majora-92bf1922-00a>.
- Ökte, E. (2002). Grow-out of sea bream *Sparus aurata* in Turkey, particularly in a land-based farm with recirculation system in Canakkale: better use of water, nutrients and space. *Turkish Journal of Fisheries and Aquatic Sciences*, 2, 83—87.
- QGIS.org (2023). *QGIS Geographic Information System*. Version: QGIS 3.28.4-Firenze, QGIS Association, <http://www.qgis.org>.
- Ravagnan, G. (1992). *Vallicoltura integrata: contributo all'acquacoltura costiera - riflessioni, analisi e proposte*. Bologna: Edagricole.
- Remen, M., Nederlof, M. A., Folkedal, O., Thorsheim, G., Sitjà-Bobadilla, A., Pérez-Sánchez, J., Oppedal, F., & Olsen, R. E. (2015). Effect of temperature on the metabolism, behaviour and oxygen requirements of *Sparus aurata*. *Aquaculture Environment Interactions*, 7, 115–123. <https://doi.org/10.3354/aei00141>.
- Schoolfield, R., Sharpe, P., & Magnuson, C. (1981). Non-linear regression of biological temperature-dependent rate models based on absolute reaction-rate theory. *Journal of Theoretical Biology*, 88, 719–731. [https://doi.org/10.1016/0022-5193\(81\)90246-0](https://doi.org/10.1016/0022-5193(81)90246-0).
- Seginer, I., & Ben-Asher, R. (2011). Optimal harvest size in aquaculture, with ras cultured sea bream (*Sparus aurata*) as an example. *Aquacultural Engineering*, 44, 55–64. <https://doi.org/10.1016/j.aquaeng.2011.03.001>.

- Song, H., Wignall, P. B., Song, H., Dai, X., & Chu, D. (2019). Seawater temperature and dissolved oxygen over the past 500 million years. *Journal of Earth Science*, *30*, 236–243. <https://doi.org/10.1007/s12583-018-1002-2>.
- Stavrakidis-Zachou, O., Lika, K., Anastasiadis, P., & Papandroulakis, N. (2021). Projecting climate change impacts on Mediterranean finfish production: a case study in Greece. *Climatic Change*, *165*, 67. <https://doi.org/10.1007/s10584-021-03096-y>.
- Virtanen, P., Gommers, R., Oliphant, T. E., Haberland, M., Reddy, T., Cournapeau, D., Burovski, E., Peterson, P., Weckesser, W., Bright, J., van der Walt, S. J., Brett, M., Wilson, J., Millman, K. J., Mayorov, N., Nelson, A. R. J., Jones, E., Kern, R., Larson, E., Carey, C. J., Polat, İ., Feng, Y., Moore, E. W., VanderPlas, J., Laxalde, D., Perktold, J., Cimrman, R., Henriksen, I., Quintero, E. A., Harris, C. R., Archibald, A. M., Ribeiro, A. H., Pedregosa, F., van Mulbregt, P., & SciPy 1.0 Contributors (2020). SciPy 1.0: Fundamental Algorithms for Scientific Computing in Python. *Nature Methods*, *17*, 261–272. <https://doi.org/10.1038/s41592-019-0686-2>.
- Wells, M. L., Trainer, V. L., Smayda, T. J., Karlson, B. S., Trick, C. G., Kudela, R. M., Ishikawa, A., Bernard, S., Wulff, A., Anderson, D. M. et al. (2015). Harmful algal blooms and climate change: Learning from the past and present to forecast the future. *Harmful algae*, *49*, 68–93. <https://doi.org/10.1016/j.hal.2015.07.009>.
- White, P. (2013). Environmental consequences of poor feed quality and feed management. In *On-farm feeding and feed management in aquaculture. FAO Fisheries Technical Paper. No. 583* (pp. 553–564). Rome: Food and Agriculture Organization of the United Nations.
- Zoli, M., Rossi, L., Costantini, M., Bibbiani, C., Fronte, B., Brambilla, F., & Bacenetti, J. (2023). Quantification and characterization of the environmental impact of sea bream and sea bass production in Italy. *Cleaner Environmental Systems*, *9*, 100118. <https://doi.org/10.1016/j.cesys.2023.100118>.

# Supplementary Information

**Article:** Effects of climate change on gilthead seabream aquaculture in the Mediterranean

**Authors:** Ines Haberle, Domagoj K. Hackenberger, Tamara Djerdj, Lav Bavčević, Sunčana Geček, Branimir K. Hackenberger, Nina Marn, Jasminka Klanjšček, Marija Purgar, Jadranka Pečar Ilić, and Tin Klanjscek

**Data Availability:** The data and code underlying the findings of this study are openly available at Zenodo, <https://doi.org/10.5281/zenodo.8325033>.

Summary of model specifications and results across figures and tables for easier navigation.

## Dynamic Energy Budget model

DEB model equations	Table A.1
DEB parameters	Table A.2

## Simulations of all indices (absolute values)

Scenario	Period		
	2021-2023	2051-2053	2091-2093
RCP 4.5	Fig. B.1	Fig. B.2	Fig. B.3
RCP 8.5	Fig. B.4	Fig. B.5	Fig. B.6

## Change of indices in mid-term (2051-2021) and long-term (2091-2021) for both RCP scenarios

Average two-year temperature	Fig. 1
Number of days exceeding 28 °C	Fig. 2
Time to market	Fig. 3
FCR at time-to-market	Fig. 4
FCR at two years	Fig. 5
Weight at two years	Fig. 6
Mid-term change between RCP 8.5 in relation to RCP 4.5 baseline	Fig. C.1

## A Dynamic Energy Budget model of gilthead seabream (*Sparus aurata*)

The fish growth model used in this study was developed using Dynamic Energy Budget (DEB) theory. This theory describes how organisms acquire and use energy for maintenance, growth and reproduction throughout their whole life cycle, while accounting for the environment conditions (Jusup et al., 2017; Kooijman, 2010; Sousa et al., 2008). Conceptually, the DEB theory divides the organism into two parts, represented by two state variables: structure ( $V$ ) and reserve ( $E$ ). A structure is a part of an organism that reflect its growth in size and requires energy expenditure for maintenance. Reserve does not require energy for maintenance, and serves as a source of energy for all physiological processes. Two additional state variables are introduced to correspond with the increase in complexity of the organism, i.e. maturation ( $E_H$ ), and energy invested towards reproduction, i.e. reproduction buffer ( $E_R$ ). The dynamics of state variables is defined by the energy fluxes: ingestion, assimilation, growth, maturation, maintenance, and reproduction. Model equations are given in the Table A.1. The fluxes depend on the species-specific DEB primary parameters that can be determined based on empirical data through a parameterization process, using freely available DEBtool software package (DEBtool, 2023; Lika et al., 2011; Marques et al., 2018). We used the typified *abj* DEB model designed for organisms undergoing metamorphosis, including fish (Kooijman et al., 2011; Marques et al., 2018). This model account for a metabolic acceleration during the larval phase, accounted for by an additional parameter, acceleration factor (Kooijman, 2014). This factor increases from birth up to metamorphosis, and stays constant afterwards, multiplying the rates of assimilation and energy conductivity throughout the life cycle. Further details on DEB theory and models are available in the corresponding literature (Jusup et al., 2017; Kooijman, 2010, 2014; Lika et al., 2011; Marques et al., 2018; Sousa et al., 2008).

The initial parameter set for the gilthead seabream was taken from the Add-my-Pet collection of DEB parameters (AmP, 2023; Lika & Kooijman, 2016), and was further refined using the gilthead seabream growth data provided confidentially by an aquaculture farm in Croatia. The final parameter set used for the simulations is given in Table A.2. In addition to primary parameters, a set of auxiliary parameters was used to relate DEB

quantities to the observable metrics such as physical weight of the organism.

We calculated FCR in terms of energy. In common, actual weight-based, FCR calculation, difference in energy and water content of feed used by aquaculture facilities can decrease comparability of the calculated FCR values. Although not recognized yet, FCR in terms of energy ( $FCR_{en}$ ) offers more universal approach than one calculated from weight - it does not depend on water content of feed, and can give more realistic insights into how much feed energy is actually converted into energy contained in the produced fish biomass.

By assuming that the fish is given all the feed it requires to achieve the modelled energy intake, and not more (to avoid waste), the amount of total ingested feed throughout the rearing process ( $X$ ) was calculated by adding up daily ingestion,  $p_X$  (Joules). The fish energy gain ( $Fish_{en}$ ) was calculated by subtracting the energy of the stocking fish from the energy of the harvested fish, i.e. sum of the energy contained in structure ( $V$ ), reserve ( $E$ ), and reproductive buffer ( $E_R$ ), at time-to-market, and after two years:

$$Fish_{en} = (d_V V \frac{\mu_V}{\omega_V} + E + E_R) - (d_V V_{init} \frac{\mu_V}{\omega_V} + E_{init} + E_{R_{init}}) \quad (A.1)$$

where  $V_{init}$ ,  $E_{init}$ ,  $E_{R_{init}}$ , and  $V$ ,  $E$ ,  $E_R$ , are the structure, reserve, and reproduction buffer of stocking and harvested fish, respectively;  $d_V$ ,  $\mu_V$ , and  $\omega_V$  are volume-mass-energy couplers to convert structural volume into energy. The FCR in terms of energy was then calculated as:

$$FCR_{en} = \frac{X}{Fish_{en}}. \quad (A.2)$$

Table A.1: General equations of the Dynamic Energy Budget (DEB) model describing energy fluxes, dynamics of state variables, and translation into physical weight. Parameters are defined in Table A.2.

### DEB energy flux

Ingestion	$\dot{p}_X = f \frac{1}{\kappa_X} \{ \dot{p}_{Am} \} s_M V^{2/3}$	(A.3)
Assimilation	$\dot{p}_A = f \{ \dot{p}_{Am} \} s_M V^{2/3}$	(A.4)
Mobilization <sup>1</sup>	$\dot{p}_C = [E] \cdot \frac{\dot{v}_{sM}[E_G]V^{2/3} + \dot{p}_S}{\kappa[E] + [E_G]}$	(A.5)
Somatic maintenance	$\dot{p}_S = [\dot{p}_M]V$	(A.6)
Maturity maintenance	$\dot{p}_J = k_J E_H$	(A.7)
Growth	$\dot{p}_G = \kappa \dot{p}_C - \dot{p}_S$	(A.8)
Maturation/Reproduction	$\dot{p}_R = (1 - \kappa) \dot{p}_C - \dot{p}_J$	(A.9)

<sup>1</sup>  $[E]$  stands for energy density,  $E/V$ .

### Dynamics of the DEB state variables

Reserve energy	$\frac{d}{dt} E = \dot{p}_A - \dot{p}_C$	(A.10)
Structural body volume	$\frac{d}{dt} V = \frac{\dot{p}_G}{[E_G]}$	(A.11)
Energy invested into maturation	$\frac{d}{dt} E_H = \dot{p}_R$ while $E_H < E_H^p$	(A.12)
Energy invested into reproduction	$\frac{d}{dt} E_R = \dot{p}_R$ when $E_H = E_H^p$	(A.13)

### Temperature correction

Correction below reference temperature ( $T < T_1$ )	$k_1 \cdot s_A(T)$	(A.14)
--	--------------------	--------

Correction above the reference temperature ( $T \geq T_1$ )	$k_1 \cdot s_A(T) \cdot s_H(T)$	(A.15)
---	---------------------------------	--------

where

$$s_A(T) = e^{T_A \left( \frac{1}{T_1} - \frac{1}{T} \right)} \quad (\text{A.16})$$

$$s_H(T) = \left( 1 + e^{T_{AH} \left( \frac{1}{T_H} - \frac{1}{T_1} \right)} \right) \cdot \left( 1 + e^{T_{AH} \left( \frac{1}{T_H} - \frac{1}{T} \right)} \right)^{-1} \quad (\text{A.17})$$

Calculation of physical wet weight	$W_w = w \left( d_V V + \frac{\omega_E}{\mu_E} (E + E_R) \right)$	(A.18)
------------------------------------	---	--------

Table A.2: Dynamic Energy Budget (DEB) model parameters for gilthead seabream. The parameters were obtained by refining the initial parameter set taken from Add-my-Pet collection (AmP, 2023; Lika & Kooijman, 2016), through a parameterisation routine using growth data. The dots above the letters denote rates, while square and curly brackets relate to volume- and surface-specific quantities, respectively. The parameters indicated in bold were fixed, i.e. were not estimated from the data. Upper temperature limit  $T_H$  is specific to gilthead seabream (Kaya Öztürk et al., 2020). The  $T_{AH}$  determining the rate of decrease in metabolic rates above  $T_H$  has been taken from the European sea bass AmP entry (Lika et al., 2018).

Primary DEB parameters	Symbol	Value	Unit
Maximal surface-specific searching rate	$\{\dot{F}_m\}$	6.73	1/d cm <sup>2</sup>
Maximal surface-specific assimilation rate	$\{\dot{p}_{Am}\}$	16.8191	J/d cm <sup>2</sup>
Fraction of food energy fixed in reserve	$\kappa_X$	0.805	–
Allocation fraction to soma	$\kappa$	0.9378	–
Fraction of reproduction energy fixed in eggs	$\kappa_R$	<b>0.95</b>	–
Energy conductance	$\dot{v}$	0.0453	cm/d
Volume-specific somatic maintenance rate	$[\dot{p}_M]$	12.5144	J/d cm <sup>3</sup>
Volume-specific costs of structure	$[E_G]$	5265.8	J/cm <sup>3</sup>
Maturity maintenance rate coefficient	$\dot{k}_J$	<b>0.002</b>	/d
Maturation threshold for birth	$E_H^b$	0.0589	J
Maturation threshold for metamorphosis	$E_H^j$	385.9	J
Maturation threshold for sexual maturation	$E_H^p$	184100	J

Temperature related parameters	Symbol	Value	Unit
Arrhenius temperature	$T_A$	8414	K
Arrhenius temperature at the upper boundary	$T_{AH}$	<b>84842</b>	K
Upper boundary of the temperature tolerance range	$T_H$	<b>301.15 (28)</b>	K (°C)
Reference temperature	$T_1$	<b>293.15 (20)</b>	K (°C)

Auxiliary DEB parameters	Symbol	Value	Unit
Shape coefficient	$\delta_M$	0.2525	–
Specific density of structure	$d_V$	<b>0.2</b>	g/cm <sup>3</sup>
	$\omega_E$	<b>23.9</b>	g/mol
Mass-energy-weight couplers <sup>†</sup>	$\mu_E$	<b>550000</b>	J/mol
	$\omega_V$	<b>23.9</b>	g/mol
	$\mu_V$	<b>500000</b>	J/mol
Wet/dry weight coefficient of fish	$w$	<b>5</b>	–
Acceleration factor <sup>¶</sup>	$s_M$	$\min(\frac{L}{L_b}, \frac{L_j}{L_b})$	–

<sup>†</sup> The subscripts indicate correspondence of parameter to: E - reserve, V - structure.

<sup>¶</sup> Acceleration factor changes with size up to metamorphosis, and is calculated as a ratio of current size  $L$  to the size at birth  $L_b$ ,  $\frac{L}{L_b}$ . It stays equal to  $\frac{L_j}{L_b}$  after metamorphosis, where  $L_j$  is size at metamorphosis. Note that  $L_* = V_*^{1/3}$ , where \* corresponds to birth (b) or metamorphosis (j).

## B Model simulations

Model simulations were performed for two IPCC RCP scenarios, 4.5 and 8.5, for three rearing periods starting in 2021, 2051, and 2091 - 6 simulations in total. For each simulation we recorded six indices, specifically (i) two aggregate environmental indicators - mean two-year temperature, and number of days exceeding 28 °C, and (ii) four aquaculture performance indicators - time-to-market, weight at two years, FCR at time-to-market, and FCR at two years. The results are presented in the Figs. B.1 to B.6. The results of these simulations were used to calculate the differences presented in the main text.

As expected, maximal value of biennial, i.e. two-year, average temperature shows a generally increasing trend as we move from reference to mid- and long-term projection period. Minimum biennial average temperature also increases, but interestingly, the minimum average of the mid-term RCP 4.5 is greater comparing to the RCP 8.5 scenario in the same period. This is however compensated by the subsequent warming in the long-term, with simulations for the RCP 8.5 scenario showing 1.1 °C higher minimum biennial average temperature compared to the long-term RCP 4.5 simulation. Number of days exceeding 28 °C also shows increasing trend, both within, and between the scenarios, with the RCP 8.5 simulations having more warmer days.

The maximal value for time-to-market decreases within the RCP 4.5 scenario from reference period throughout the mid- and long-term, while this index increases in the mid-term, but sharply decreases for the long-term RCP 8.5 simulations. The same is observed for the lowest time-to-market value. As expected, the exact opposite trend is obtained for weight after a two-year rearing process, i.e within the scenario, it increases for the RCP 4.5 scenario (with the exception of long-term scenario which is slightly lower compared to the mid-term), and decreases in the mid-term RCP 8.5, compensated by the sharp increase in the long-term.

The minimal and maximal FCR values do not show any greater change between mid- and long-term simulations, as well as between RCP scenarios, with the average value staying at 2.13 for all simulations. The FCR at two-years for the RCP 4.5 scenario shows a slight increase from reference period to long-term simulation, with higher minimum, maximum, and average value for the latter. For the RCP 8.5 scenario, the minimum, maximum, and average value of the two-year FCR decrease in the mid-term, but increase in the long-term period.

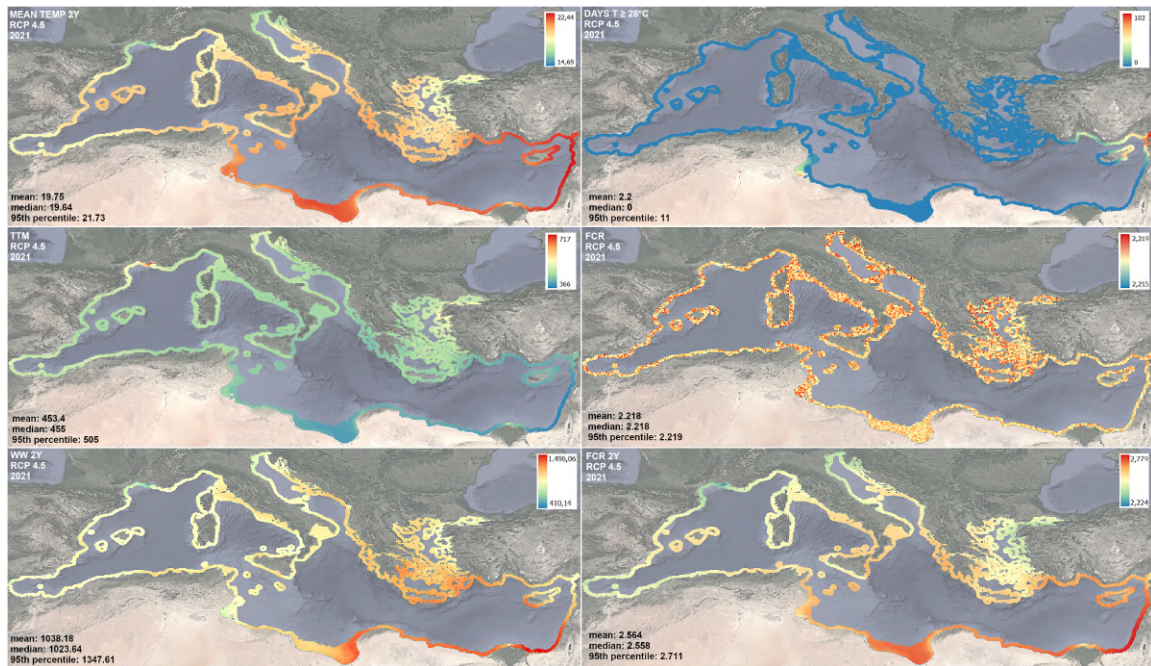


Figure B.1: Simulations of six indices for the rearing period 2021-2023 under the RCP 4.5 climate change scenario. Left: average two-year temperature, time-to-market, weight at two-years; Right: number of days exceeding 28 °C, FCR at time-to-market, FCR at two-years. Mean, median, and 95<sup>th</sup> percentile change are indicated in the lower left corner of each plot.

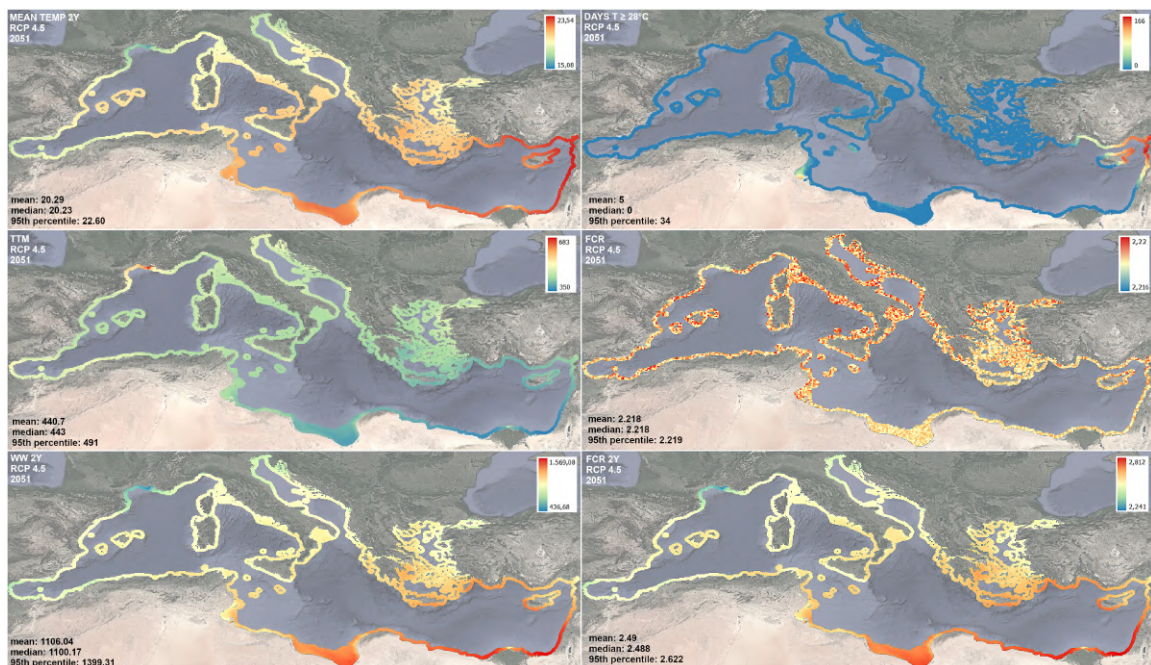


Figure B.2: Simulations of six indices for the rearing period 2051-2053 under the RCP 4.5 climate change scenario. Left: average two-year temperature, time-to-market, weight at two-years; Right: number of days exceeding 28 °C, FCR at time-to-market, FCR at two-years. Mean, median, and 95<sup>th</sup> percentile change are indicated in the lower left corner of each plot.

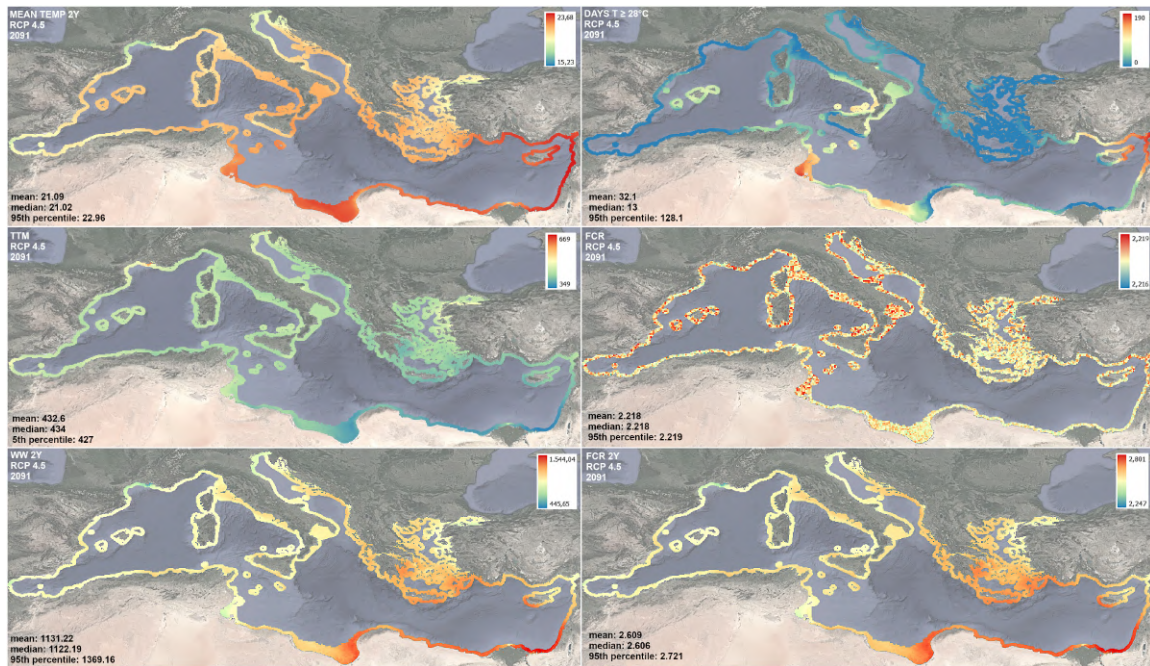


Figure B.3: Simulations of six indices for the rearing period 2091-2093 under the RCP 4.5 climate change scenario. Left: average two-year temperature, time-to-market, weight at two-years; Right: number of days exceeding 28 °C, FCR at time-to-market, FCR at two-years. Mean, median, and 95<sup>th</sup> percentile change are indicated in the lower left corner of each plot.

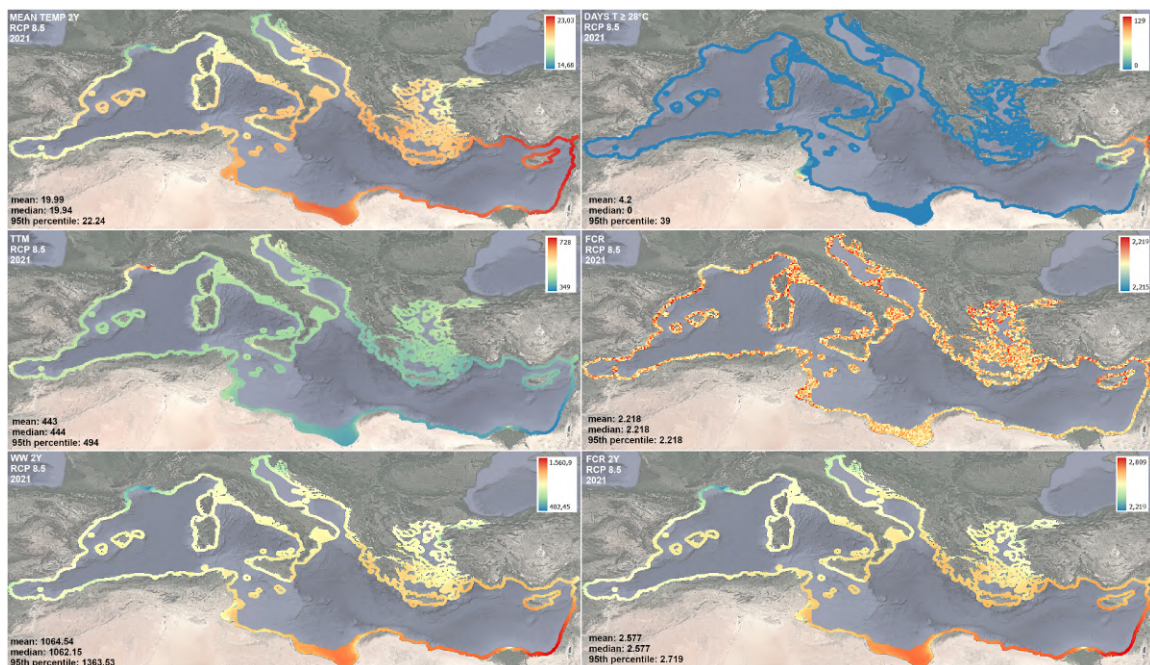


Figure B.4: Simulations of six indices for the rearing period 2021-2023 under the RCP 8.5 climate change scenario. Left: average two-year temperature, time-to-market, weight at two-years; Right: number of days exceeding 28 °C, FCR at time-to-market, FCR at two-years. Mean, median, and 95<sup>th</sup> percentile change are indicated in the lower left corner of each plot.

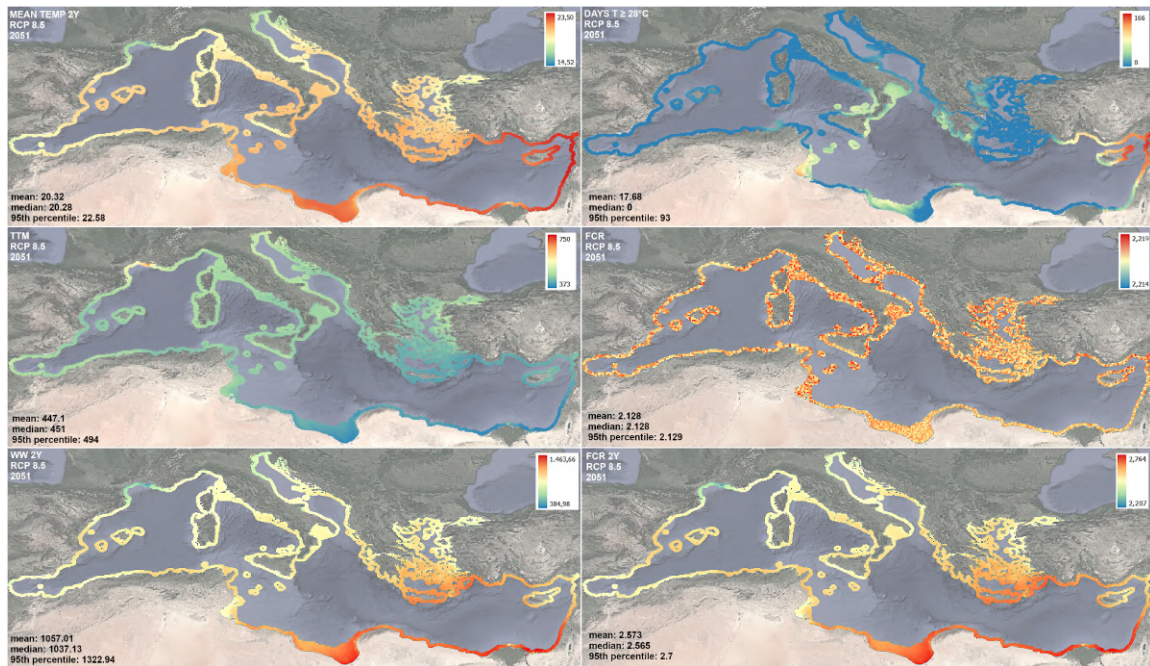


Figure B.5: Simulations of six indices for the rearing period 2051-2053 under the RCP 8.5 climate change scenario. Left: average two-year temperature, time-to-market, weight at two-years; Right: number of days exceeding 28 °C, FCR at time-to-market, FCR at two-years. Mean, median, and 95<sup>th</sup> percentile change are indicated in the lower left corner of each plot.

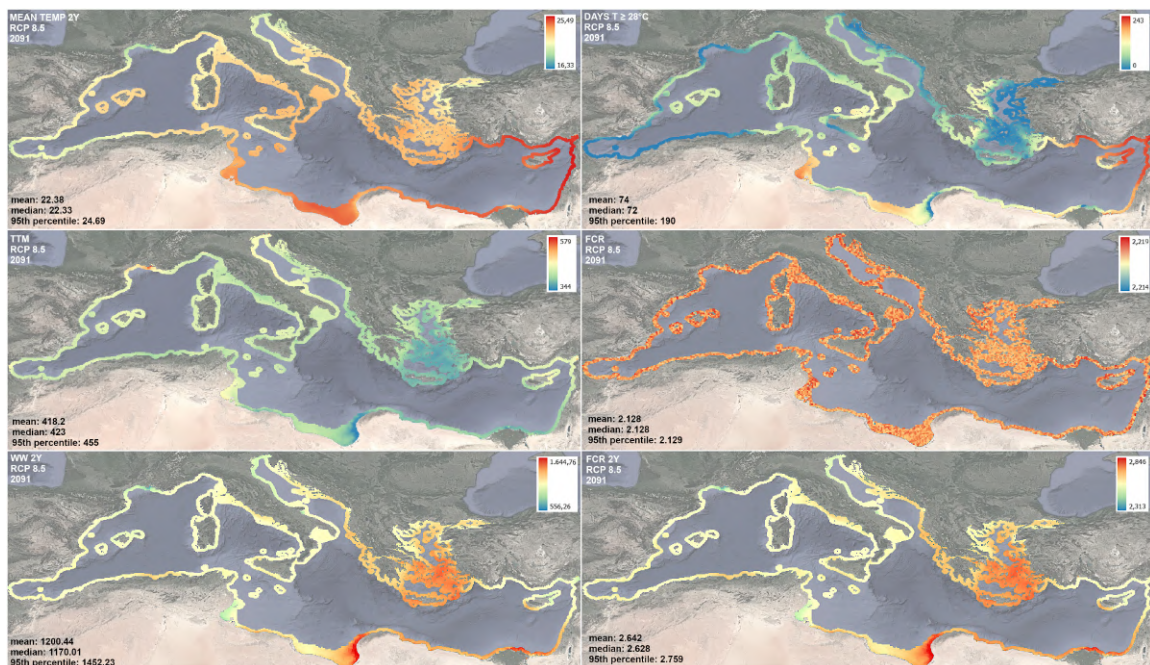


Figure B.6: Simulations of six indices for the rearing period 2091-2093 under the RCP 8.5 climate change scenario. Left: average two-year temperature, time-to-market, weight at two-years; Right: number of days exceeding 28 °C, FCR at time-to-market, FCR at two-years. Mean, median, and 95<sup>th</sup> percentile change are indicated in the lower left corner of each plot.

## C Impact of projections for baseline temperature

Note that temperature data of the reference time period (2021-2023) are projections rather than actual measurements. Therefore, temperatures during the reference period differ between the two RCP scenarios, i.e. baselines differ as well. Fig. C.1 illustrates the point: when RCP 4.5 baseline is used for estimating mid-term changes in RCP 8.5, climate change effects are indeed greater than those predicted for RCP 4.5 (top left panels in Figs. 1 to 6 in the main text).

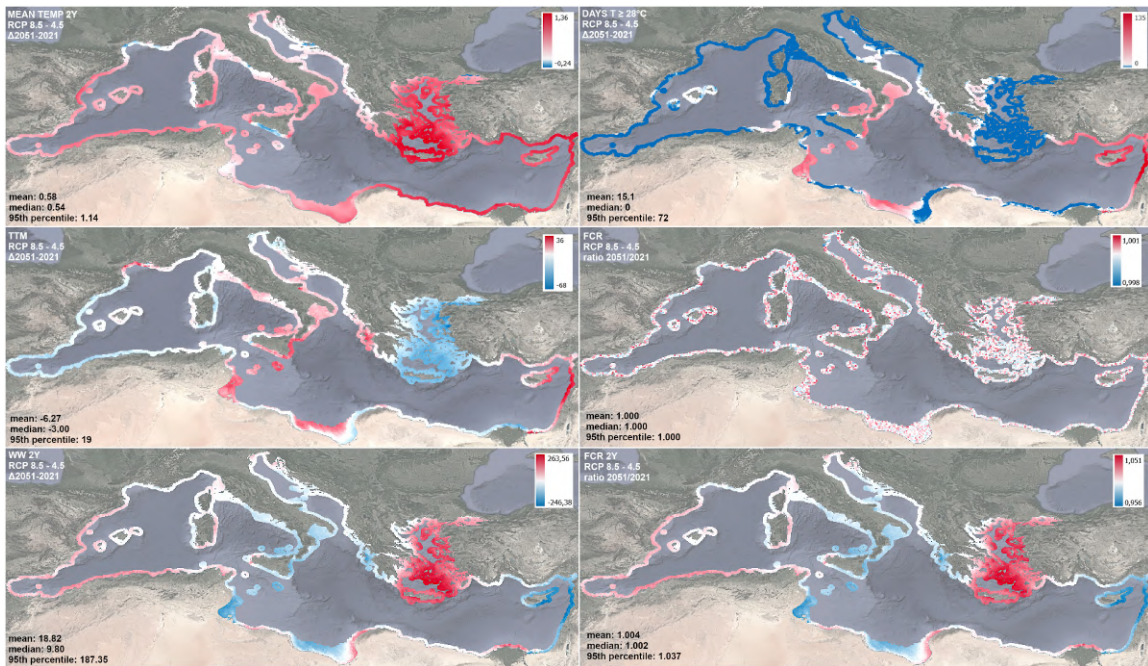


Figure C.1: Changes in six indices between the RCP 4.5 reference rearing period (2021-2023) and the RCP 8.5 mid-term rearing period (2051-2053). Difference in FCR is expressed relative to the reference period; other indices are expressed as differences in absolute values. Mean, median, and 95<sup>th</sup> percentile change are indicated in the lower left corner of each plot.

## References

- AmP (2023). Add-my-Pet collection. [https://www.bio.vu.nl/thb/deb/deblab/add\\_my\\_pet/species\\_list.html](https://www.bio.vu.nl/thb/deb/deblab/add_my_pet/species_list.html). Accessed on 30.04.2023.
- DEBtool (2023). Software package DEBtool\_M. [https://github.com/add-my-pet/DEBtool\\_M](https://github.com/add-my-pet/DEBtool_M).
- Jusup, M., Sousa, T., Domingos, T., Labinac, V., Marn, N., Wang, Z., & Klanjšček, T. (2017). Physics of metabolic organization. *Physics of Life Reviews*, 20, 1–39. <https://doi.org/10.1016/j.plrev.2016.09.001>.
- Kaya Öztürk, D., Öztürk, R., Baki, B., Karayücel, I., & Karayücel, S. (2020). Monthly variation of growth, biochemical composition, fatty and amino acids patterns of gilthead sea bream (*Sparus aurata*) in offshore cage systems under brackish water conditions in the Black Sea. *Aquaculture Research*, 51, 4961–4983. <https://doi.org/10.1111/are.14833>.
- Kooijman, S., Pecquerie, L., Augustine, S., & Jusup, M. (2011). Scenarios for acceleration in fish development and the role of metamorphosis. *Journal of sea research*, 66, 419–423. <https://doi.org/10.1016/j.seares.2011.04.016>.
- Kooijman, S. A. L. M. (2010). *Dynamic Energy Budget theory for metabolic organisation*. Cambridge: Cambridge University Press.
- Kooijman, S. A. L. M. (2014). Metabolic acceleration in animal ontogeny: an evolutionary perspective. *Journal of Sea Research*, 94, 128–137. <https://doi.org/10.1016/j.seares.2014.06.005>.
- Lika, D., & Kooijman, B. (2016). AmP *Sparus aurata*, version 2016/10/15. [https://www.bio.vu.nl/thb/deb/deblab/add\\_my\\_pet/entries\\_web/Sparus\\_aurata/Sparus\\_aurata\\_res.html](https://www.bio.vu.nl/thb/deb/deblab/add_my_pet/entries_web/Sparus_aurata/Sparus_aurata_res.html). Accessed on 30.04.2023.
- Lika, D., Kooijman, B., & Stavrakidis Zachou, O. (2018). AmP *Dicentrarchus labrax*, version 2018/05/11. [https://www.bio.vu.nl/thb/deb/deblab/add\\_my\\_pet/entries\\_web/Dicentrarchus\\_labrax/Dicentrarchus\\_labrax\\_res.html](https://www.bio.vu.nl/thb/deb/deblab/add_my_pet/entries_web/Dicentrarchus_labrax/Dicentrarchus_labrax_res.html). Accessed on 03.05.2023.
- Lika, K., Kearney, M. R., Freitas, V., van der Veer, H. W., van der Meer, J., Wijsman, J. W., Pecquerie, L., & Kooijman, S. A. L. M. (2011). The “covariation method” for estimating the parameters of the standard dynamic energy budget model I: Philosophy and approach. *Journal of Sea Research*, 66, 270–277. <https://doi.org/10.1016/j.seares.2011.07.010>.
- Marques, G. M., Augustine, S., Lika, K., Pecquerie, L., Domingos, T., & Kooijman, S. A. L. M. (2018). The AmP project: Comparing species on the basis of dynamic energy budget parameters. *PLoS Computational Biology*, 14, 1–23. <https://doi.org/10.1371/journal.pcbi.1006100>.
- Sousa, T., Domingos, T., & Kooijman, S. (2008). From empirical patterns to theory: a formal metabolic theory of life. *Philosophical Transactions of the Royal Society B: Biological Sciences*, 363, 2453–2464. <https://doi.org/10.1098/rstb.2007.2230>.